YC Diwu et al. J Brain Disord 2017, 1(1):25-34
DOI: 10.36959/524/327 | Volume 1 | Issue 1

Journal of Brain Disorders

Research Article Open Access

Effect of Chinese Herbal Medicine Xixin Decoction on Aβ42 and its Regulatory Enzymes in APP/PS1 Double Transgenic Murine Brain

Diwu Yong-chang[1]*, Gu Zan[1], Cui Na[2], Yang Ke[1], Gu Jie[3], Zeng Jian[1], Li Xiang[1], Gao Yan-bin[1], Tang Xue-cheng[1] and Zhai Jia-ming[1]

[1]*The First Clinical Medical College, Shaanxi University of Chinese Medicine, China*

[2]*The College of Foreign Languages, Shaanxi University of Chinese Medicine, China*

[3]*The Medical Research Center, Shaanxi University of Chinese Medicine, China*

Abstract

Objective: To observe the effect of a Xixin decoction on learning and memory in APP/PS1 transgenic mice in addition to hippocampal ultrastructure and hippocampal Aβ42 related regulatory enzymes.

Methods: APP/PS1 double transgenic mice were randomly divided into three groups: Model, Aricept, and Xixin decoction. Controls were APP/PS1 negative, C57BL/6J littermates. All groups received intragastric gavage for three months after which they were subjected to the Morris water maze and other behavioral testing. After irradiation, mice were decapitated and resulting tissue examined using electron microscopy, immunofluorescence, and Western blot to observe ultrastructural changes to hippocampal neurons and protein expression levels of Aβ42, BACE, and IDE.

Results: Compared with the Model group, the Xixin decoction group had significantly shortened average escape latencies ($P < 0.05$). When comparing Xixin decoction with the Model group, both Aβ42 and BACE protein expression were significantly reduced ($P < 0.05$) while IDE expression was significantly increased ($P < 0.05$). Conclusion: Treatment with Xixin had good effects on the learning and memory abilities of APP/PS1 transgenic mice. Xixin treatment also had protective effects on the structure, morphology, and functioning of hippocampal neurons and synapses in APP/PS1 double transgenic mice. Importantly, Xixin decoction effectively reduced Aβ42 content in APP/PS1 transgenic murine brain and inhibited the over-expression of BACE that promoted IDE expression.

Keywords

Alzheimer's disease, Xixin decoction, Amyloid beta protein, β-secretase enzyme, Insulin degrading enzyme

Introduction

Alzheimer's Disease (AD) is a neurodegenerative disease that has an insidious onset and slow progression [1]. Despite the vast amount of work done on AD, its pathogenesis is still unclear, resulting in a lack of specific treatments. This deficit is currently a large focus for both Traditional Chinese Medicine (TCM) as well as Western medical research. Although a clear mechanism for AD is still missing, the current "Aβ cascade" theory is a core component of current thinking regarding AD pathogenesis [2]. One school of thought holds that β-amyloid (Aβ) aggregation is a key mechanism in AD pathogenesis, with Aβ accumulation and deposition in the brain being one of the main pathological changes in AD patients. Further work has confirmed that the occurrence of Aβ accumulation results in neurotoxicity, synaptic injury, and neuronal death [3]. Aβ is produced

***Corresponding author:** Diwu Yong-chang, The First Clinical Medical College, Shaanxi University of Chinese Medicine, Century Avenue, Xi'an-Xianyang, Shaanxi Province, Shaanxi 712046, China, Tel: 029-38183462, E-mail: diwuyongchang@126.com

Received: October 28, 2016; **Accepted:** June 14, 2017; **Published online:** June 16, 2017

Citation: YC Diwu, Zan G, Na C, et al. (2017) Effect of Chinese Herbal Medicine Xixin Decoction on Aβ42 and its Regulatory Enzymes in APP/PS1 Double Transgenic Murine Brain. J Brain Disord 1(1):25-34

by the continuous action of β-protease and γ-protease decomposition [4]. As a result, $A\beta_{42}$ becomes a key factor in the amyloid plaque nuclear process. The β-Site Amyloid Precursor Protein-Cleaving Enzyme 1 (BACE1) has been recognized as playing a major role in β-secretase activities, as it hydrolyzes amyloid digestion to produce $A\beta_{42}$ [5]. To this end, Insulin-Degrading Enzyme (IDE) can reduce the balance of Aβ levels, thereby reducing Aβ aggregation [6], which can regulate brain Aβ production and clearance. To this end, the work presented here sought to explore the effect of Xixin decoction on the learning and memory abilities of APP/PS1 double transgenic mice as well as hippocampal ultrastructure and brain levels of $A\beta_{42}$. We also sought to understand its effect on the expression and regulation BACE and IDE, to explore possible mechanisms and future treatment options for AD.

Materials and Methods

Drugs

The Xixin decoction was composed of ginseng, fushen, spine date seed, pinellia, dried orange peel, medicated leaven, monkshood, Acorus gramineus, and licorice. Preparation of Xixin Decoction using the corresponding proportion of non-boiling granules. The granules used were provided by Pharmaceutical Co., Ltd., Beijing Kang Rentang. Aricept was obtained in tablet form, which was provided by Eisai (China) Pharmaceutical Co., Ltd. (5 mg/tablet, batch number H20050978).

Materials and equipment

General reagents used included glutaraldehyde, paraformaldehyde, chloral hydrate, physiological saline, sucrose, sodium dihydrogen phosphate, anhydrous ethanol, acetone, citric acid sodium, glycine, Protease Inhibitors PMSF, BD skimmed milk powder, and tissue embedding medium. RIPA lysis and extraction buffer was obtained from Xi'an Science and Technology Co., Ltd. All phosphatase and protease inhibitors were obtained from Roche. Western blot reagents and equipment included HRP (ECL) light-emitting liquid (Millpore), 5 × SDS-PAGE loading buffer, SDS gel kit, BCA Protein Quantification Kit, and PVDF membranes. Primary antibodies included: Aβ42 (Cell Signaling, #14974s), BACE (Cell Signaling, #5606S), IDE (Abcam, AB2077), and all were conjugated to a FITC secondary antibody for immunofluorescence using DAPI as a counterstain (for immunofluorescence). General protein localization and quantification reagents also included an anti-quenching agent, 0.3% Tritonx-100, and 10% calf serum. Behavioral testing included the use of a Morris water maze test. In addition, this experiment also involves fluorescence microscope, electrophoresis, transfer membrane apparatus, etc.

Experimental animals and groups

APP/PS1 double transgenic mice (License No. SCXK (Su) 2015-0001) and APP/PS1 C57/B6J negative littermate controls were purchased from the Nanjing Institute of Animal Models. Experimental groups were as follows: Blank Control group (APP/PS1 C57BL/6J negative littermates), Model group (APP/PS1, double transgenic mice), Aricept group (APP/PS1 transgenic mice), and Xixin decoction group (APP/PS1 transgenic mice). All groups included 12 mice each. Animal drug delivery was calculated according to the human and mouse body surface area conversion formula to yield the unit dosage in mice. Dosages were as follows: Xixin decoction group (1.8 g/kg/d) and Aricept group (0.014 mg/kg/d). Both the model control groups received identical saline volumes. Drug administration was conducted using intragastric gavage (i.g.) for all groups and administration occurred daily for three months.

Behavioral tests

After three months' of gastric lavage, all subjects were given the Morris water maze test to assess their learning and memory. The place navigation test was used to measure the spatial learning and memory ability of the animals in the water maze. The animals were allowed to swim freely for 2 min before the test. During the test, the animals were trained twice daily each for 120 s for 5 d. A quadrant adjacent to the quadrant in which the platform is located was selected to put the mice facing the wall into the water and the time for them to find the target platform and climb up was recorded, respectively. This time span was called escape latency. Swimming distance was also recorded for each mice. If the mice did not find the platform in 120 s, it will be brought out of the water to the platform by the experimenter and stays there for 20 s. For such mice the escape latency was recorded as 120 s. Spatial probe test was used to measure the memory ability of mice for memorizing the accurate location of the platform, namely, memory retention. The mice was put into the water from any place to swim for 120 s and the crossing platform times of mice in the target quadrant (the quadrant in which the platform is located) and other quadrants was recorded, respectively.

Transmission Electron Microscopy (TEM)

After the conclusion of behavioral testing, mice were administered an intraperitoneal injection of 10% chloral hydrate aldehyde anesthesia (0.01 ml/g). They were then transcardially perfused, with sufficient exsanguination having occurred when (1) Both the liver and lung had turned white and (2) The right atrium effluent ran clear. We then used 4% polyoxymethylene as a fixative, using a hardened liver as an indicator for successful fixation. The

Table 1: Effect of Xixin decoction on the escape latency of APP/PS1 double transgenic mice (mean ± S.D., n = 12 for all groups).

Group	Day 1 (s)	Day 2 (s)	Day 3 (s)	Day 4 (s)	Day 5 (s)
Blank	51.33 ± 15.24	35.15 ± 21.26$^{\Delta}$	24.88 ± 18.05$^{\Delta}$	21.96 ± 30.23$^{\Delta}$	20.31 ± 23.07$^{\Delta}$
Model	56.25 ± 10.40	41.17 ± 19.66	40.40 ± 19.81	28.10 ± 21.92	29.23 ± 16.51
Aricept	52.98 ± 13.77	46.04 ± 19.71	35.71 ± 22.85	26.92 ± 21.92	23.00 ± 20.28
Xixin decoction	52.15 ± 13.49	36.27 ± 21.87	31.83 ± 21.01$^{\Delta}$	21.08 ± 21.96$^{\Delta}$	20.81 ± 16.84$^{\Delta}$

N.B.: Compared with the model group, $^{\Delta}P < 0.05$.

mouse was then rapidly decapitated, brain tissue harvested, and placed in glutaraldehyde for overnight fixation. After fixation, we used an ultramicrotome to cut 70 nm ultrathin sections of hippocampal tissue. We then used a JEM-1230 TEM to observe and image neuronal ultrastructure in murine hippocampal CA1, CA2, and CA3 for later analysis.

Western blot

Mice were decapitated, the hippocampi rapidly dissected, and tissue placed in the -80 °C for preservation. Tissue was lysed using RIPA lysis and extraction buffer, ultrasonically homogenized, and then centrifuged at 4 °C for 10 min at 12,000 rpm. The supernatant was extracted and subjected to protein quantification. Protein was equally loaded into gels, electrophoresed, and transferred onto a PVDF membrane. The resulting blots were then incubated at 4 °C overnight with various primary antibodies. Blots were washed briefly and then incubated with secondary antibody at room temperature for 2 h. Blots were then rinsed, incubated with ECL luminous fluid, and Optical density of each band in the image was an-alyzed via image collecting and analyzing software of digital medical image analysis system.

Immunofluorescence assay

A separate group of mice were rapidly decapitated, whole brain tissue harvested, and fixed in 4% paraformaldehyde overnight. Fixed tissue was then dehydrated by submerging in 30% sucrose at 4 °C overnight. This dehydration step was repeated twice. After dehydration, tissue was placed in a -20 °C cryostat microtome, embedded using OCT embedding medium, and cut into 4 μm sections. Sections were then incubated with various primary antibodies diluted in PBS, 4 °C overnight. Second FITC antibody incubation occurred in the dark at room temperature using an immunofluorescence antibody dilution diluent. Sections were then counterstained with the nuclear DAPI stain for approximately 5-10 min. Solution was discarded and slices were washed twice with PBS containing 0.3% triton-x100 washed (5 min per wash) followed by a final PBS was (5 min). PBS was discarded and an appropriate amount of fluorescent quenching protection liquid was then added. Slices were then mounted on slides and observed using a fluorescence microscope (Olympus 1X71).

Table 2: Average number of platform crossings per group (mean ± S.D., n = 12).

Group	Cases	Number of times through the platform	The average number of times cross platform
Blank	12	28	2.33 ± 1.15$^{\Delta}$
Model	12	14	1.17 ± 1.11
Aricept	12	23	1.92 ± 1.62
Heartwashing	12	29	2.42 ± 1.44$^{\Delta}$

N.B.: Compared with the model group, $^{\Delta}P < 0.05$.

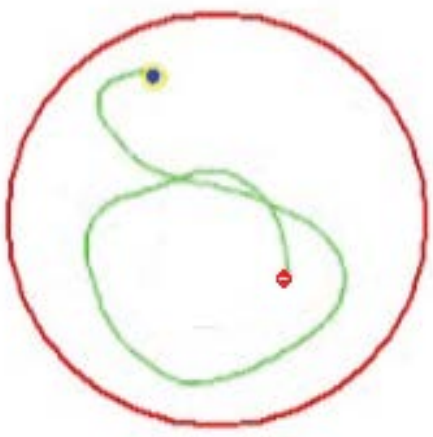

Figure 1: Blank control group's platform search route.

Statistical analysis

A commercially available statistical package (SPSS19.0) was used to analyze all data. A single factor, Analysis of Variance (ANOVA) was used to compare data between groups. A p-value less than 0.05 were considered statistically significant.

Results

Behavioral tests

Mice showed a downward trend in average escape latency with training. Starting from Day 3 and when compared with the Model group, the Xixin decoction group had significantly shortened average escape latencies ($P < 0.05$). There were no significant differences when comparing the Aricept with Xixin decoction groups ($P > 0.05$). When comparing the Model and control groups, Xixin treated mice showed significantly increased platform crossings ($P < 0.05$). There were no significant differences in platform crossings between the Aricept and

Model groups (P > 0.05) (Table 1, Table 2, Figure 1, Figure 2, Figure 3, Figure 4, Figure 5 and Figure 6).

Transmission electron microscopy

The blank control group had normal CA1 hippocampal morphology, clear structure, and unchanged organelles. Similarly, hippocampal CA2 and CA3 revealed normal cell structure, morphologically normal organelles, and only a small amount of lipofuscin (Figure 7).

The Model group revealed degeneration of hippocampal CA1 neurons, the disappearance of organelles, and evidence of mitochondrial injury (e.g. spinal frac-

Figure 2: Model group's platform search route.

Figure 3: Aricept's platform search route.

Figure 4: Xixin group's platform search route.

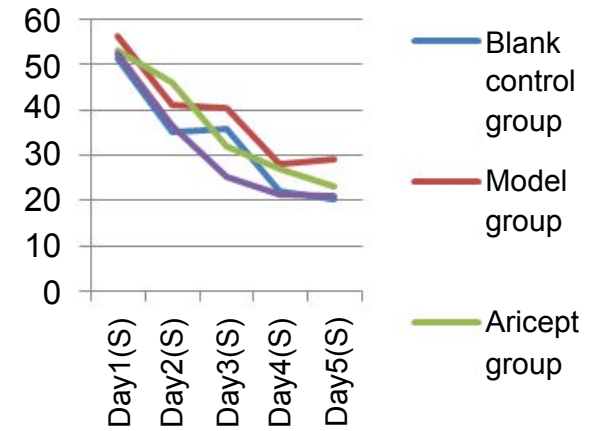

Figure 5: Escape latencies of each group.

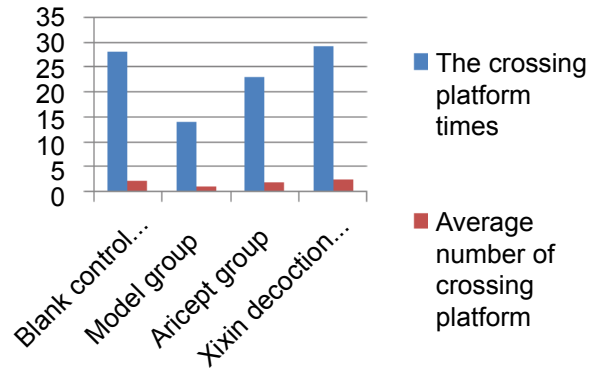

Figure 6: Platform crossings for each group.

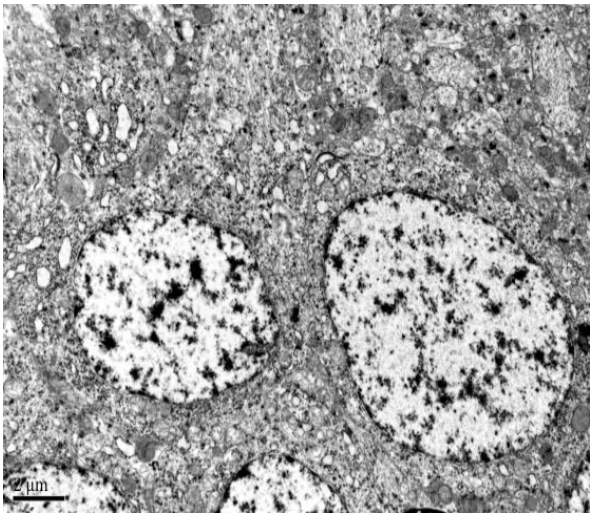

Figure 7: Blank control group.

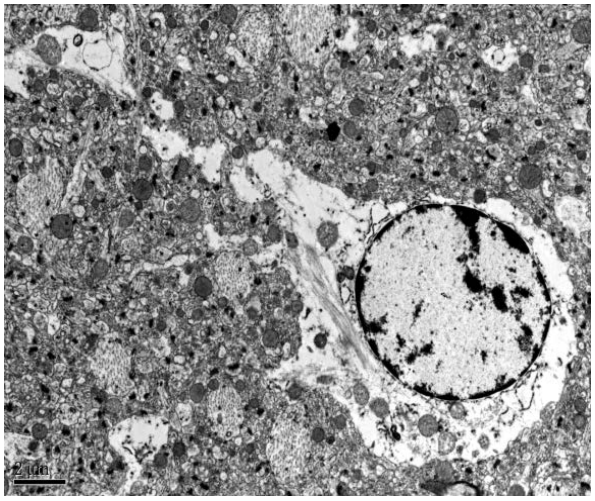

Figure 8: Model group.

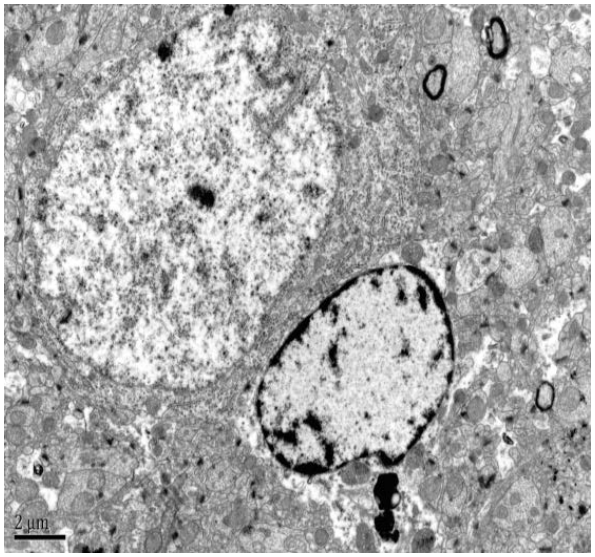

Figure 9: Aricept group.

ture). Furthermore, there was evidence of expansion of both the endoplasmic reticulum and Golgi apparatus, visible lipofuscin, and myeloid bodies. Hippocampal CA2 neurons also showed serious cellular degeneration, visible cytoplasmic myeloid bodies, and lipofuscin. There was also slight axonal degeneration, incomplete membranes, and irregular nuclei. Hippocampal CA3 neurons addicted to neural phenomena, expansion of mitochondrial ridge bubbles, irregularly shaped neuronal nuclei, and lipofuscin (Figure 8).

The Aricept group showed neuronal degeneration in the hippocampal CA1 region, including irregularly shaped nuclei and expansion of mitochondrial ridge bubbles. Both the endoplasmic reticulum and Golgi apparatus appeared to have normal morphology. Hippocampal CA2 and CA3 neurons showed significant mitochondrial swelling and a small amount of lipofuscin.

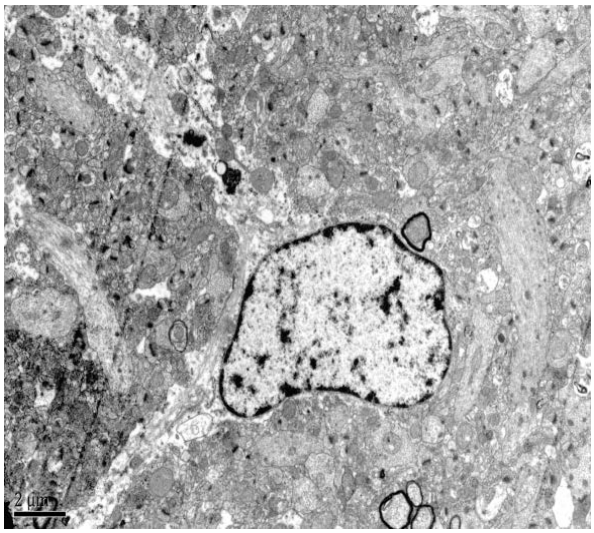

Figure 10: Xixin decoction.

Table 3: Aβ42 protein levels in all groups (ID/βactin).

Group	n	Gray-scale %
Blank group	6	56.01 ± 7.05$^{\Delta}$*
Model group	6	74.26 ± 9.02
Aricept group	6	72.08 ± 5.92
Xixin decoction group	6	63.25 ± 8.06$^{\Delta}$*

N.B.: Compared with the model and aricept groups, $^{\Delta}$*P < 0.05.

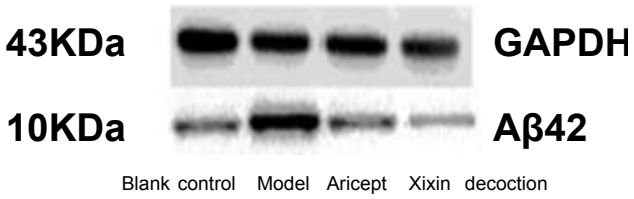

Figure 11: Aβ42 protein bands.

Finally, both CA2 and CA3 regions showed glial cell degeneration (Figure 9).

The Xixin decoction group had slight CA1 hippocampal neuronal degeneration, dissolved and degenerated mitochondrial vesicles, and normal looking endoplasmic reticulum and Golgi apparatus. CA2 neurons had slight degeneration, the presence of neuronophagia, visible lipofuscin, and slight mitochondrial degeneration (Figure 10).

Western blot

Aβ42: When compared with the Control group, mice in the Model group showed significantly increased levels of Aβ42 ($P < 0.05$). When compared with the Model group, Xixin decoction group had significantly decreased levels of Aβ42 ($P < 0.05$). Neither the Model nor the Aricept groups had significant differences in Aβ42 levels ($P > 0.05$). Finally, Aricept group compared to Xixin decoction group Aβ42 levels were significantly decreased ($P < 0.05$) (Table 3, Figure 11 and Figure 12).

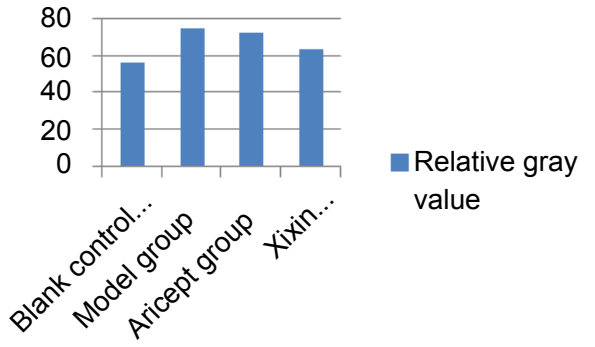

Figure 12: Aβ42 levels across groups.

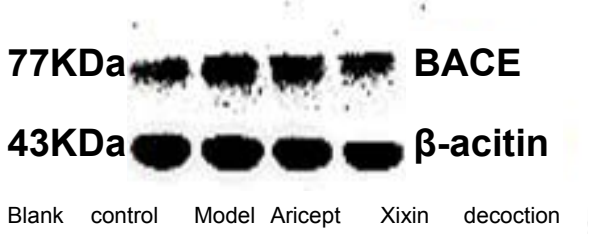

Figure 13: BACE protein bands in each group.

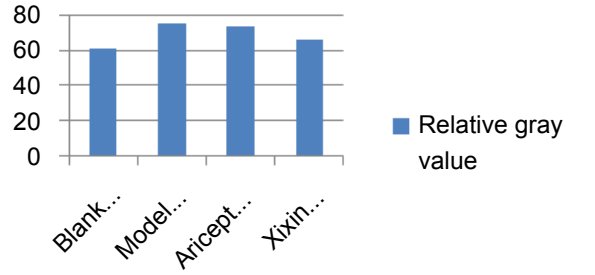

Figure 14: Hippocampal BACE expression.

Table 4: BACE protein expression levels (ID/β-actin).

Group	n	Average absorbance
Blank group	6	60.98 ± 4.47$^{\Delta *}$
Model group	6	74.58 ± 3.19
Aricept group	6	73.31 ± 2.26
Xixin decoction group	6	65.28 ± 7.48$^{\Delta *}$

N.B.: Compared with the model group; $^{\Delta}P < 0.05$ compared with the aricept group; *P < 0.05.

BACE: When compared with the Control group, the model group showed significantly increased levels of BACE ($P < 0.05$). When compared with the Model group, the Xixin decoction group had significant decreased BACE expression ($P < 0.05$). There were no significant differences in BACE expression between either the Model or Aricept groups ($P > 0.05$). Finally, BACE expression was significantly reduced in the Aricept group when compared to the Xixin decoction group ($P < 0.05$) (Table 4, Figure 13 and Figure 14).

IDE: When compared with the Blank and Model groups, IDE protein expression was significantly decreased ($P < 0.01$). When compared with the Model group, IDE protein expression in the Xixin decoction group was significantly increased ($P < 0.01$). When compared with the Model group, IDE protein expression in the Aricept group was significantly increased ($P < 0.05$). Finally, there was a significant increase in IDE expression when comparing the Aricept group with the Xixin decoction group ($P < 0.05$) (Table 5, Figure 15 and Figure 16).

Table 5: IDE protein expression levels (ID/β-actin).

Group	n	Grey-scale percentage
Blank group	6	92.420 ± 7.535$^{\Delta\Delta}$
Model group	6	68.524 ± 8.233
Aricept group	6	80.005 ± 9.045$^{\Delta}$
Xixin decoction group	6	95.770 ± 8.758$^{\Delta\Delta *}$

N.B.: Compared with the model group, $^{\Delta\Delta}P < 0.01$, $^{\Delta}P < 0.05$; Compared with the aricept group, *P < 0.05.

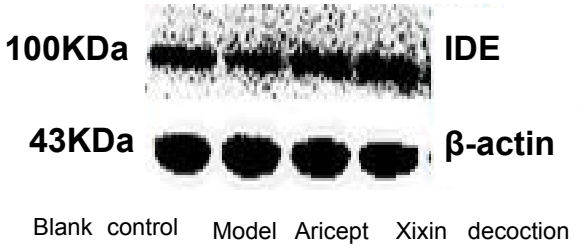

Figure 15: IDE protein bands in each group.

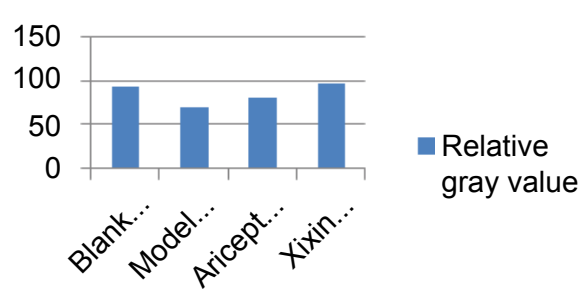

Figure 16: Hippocampal IDE expression.

Immunofluorescence

Aβ-42: When compared with the Blank Control group, the Model group had an increase in Aβ42 fluorescence. When compared with the Model group, the Xixin decoction group had a marked decrease in Aβ42 fluorescence. When compared with the Model group, the Aricept group had no significant differences in Aβ42 fluorescence. When compared with the Aricept group, the Xixin decoction group showed a marked decrease in Aβ42 fluorescence (Figure 17, Figure 18, Figure 19 and Figure 20).

BACE: When compared with the Blank Control group,

Figure 17: Control group Aβ42 immunofluorescence.

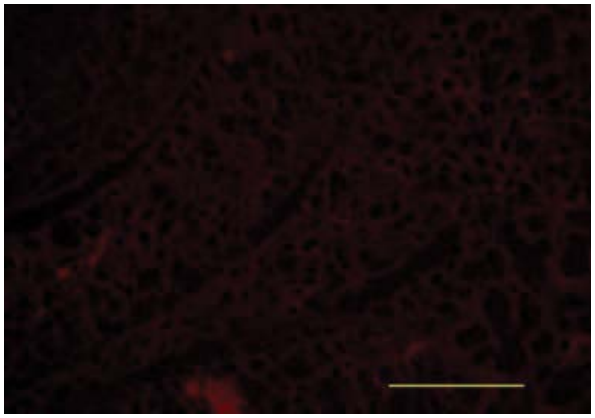

Figure 18: Model group Aβ42 immunofluorescence.

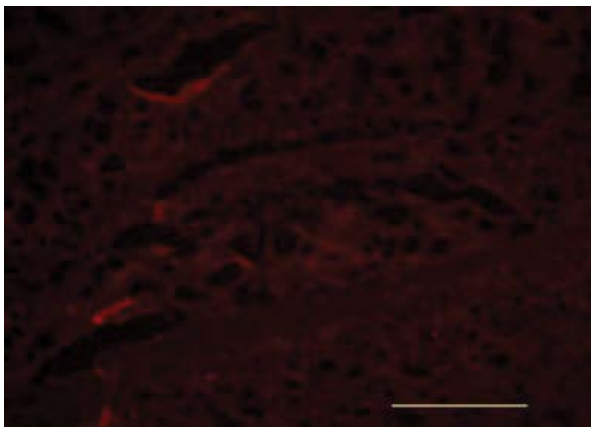

Figure 19: Aricept group Aβ42 immunofluorescence.

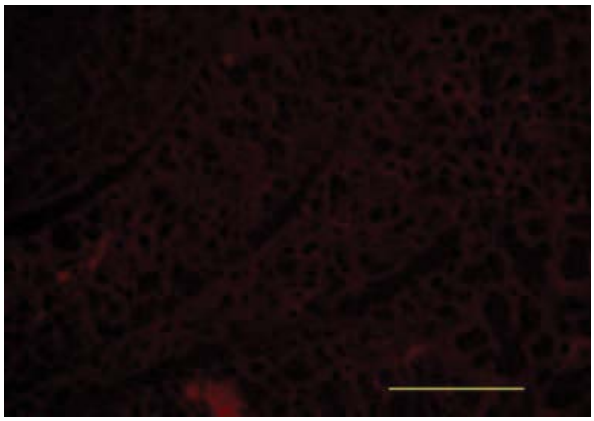

Figure 20: Xixin decoction group Aβ42 immunofluorescence.

Figure 21: Control group BACE immunofluorescence.

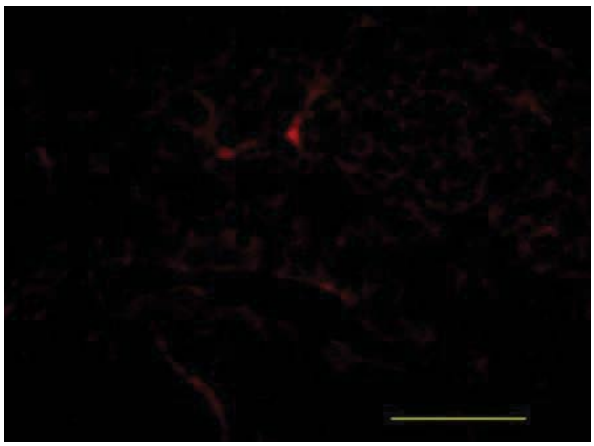

Figure 22: Model group BACE immunofluorescence.

the Model group showed a marked increase in was BACE fluorescence. When compared with the Model group, the Xixin decoction group showed a decrease in BACE fluorescence. When compared with the Model group, the Aricept group showed no notable differences in BACE fluorescence. When compared with the Aricept group, there was a marked decrease in BACE fluorescence in the Xixin decoction group (Figure 21, Figure 22, Figure 23 and Figure 24).

IDE: When compared with the Blank Control group, the Model group showed a markedly decreased IDE protein fluorescence. When compared with the Model group, the Aricept group showed an increase in IDE fluorescence. There were no differences in IDE fluorescence between the Aricept and Xixin decoction groups (Figure 25, Figure 26, Figure 27 and Figure 28).

Discussion

Aβ is thought to be a core factor in the pathogenesis

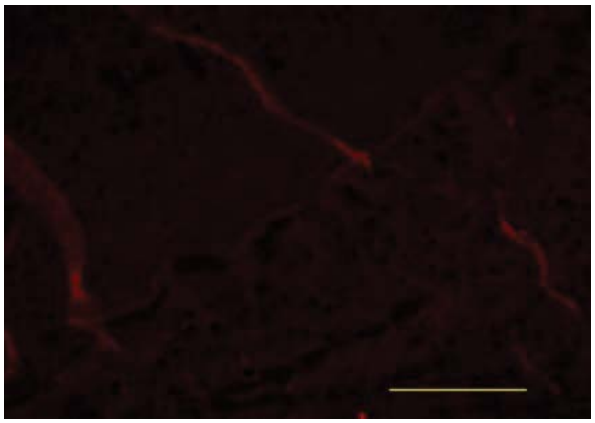

Figure 23: Aricept group BACE immunofluorescence.

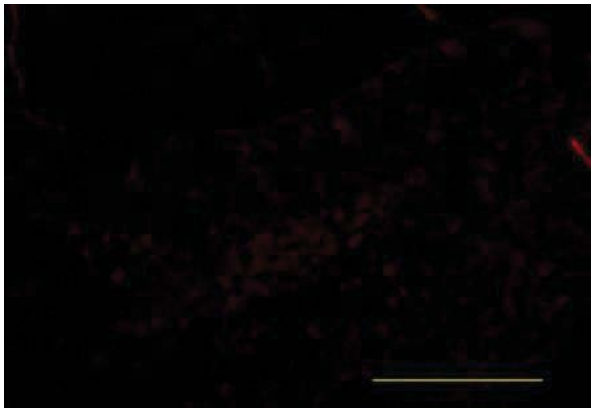

Figure 24: Xixin decoction group BACE immunofluorescence.

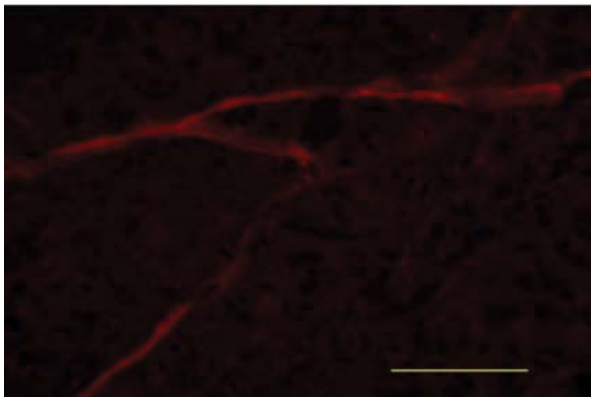

Figure 25: Control group IDE immunofluorescence.

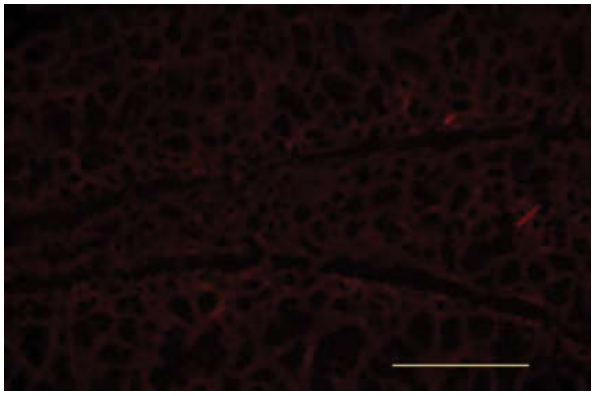

Figure 26: Model group IDE immunofluorescence.

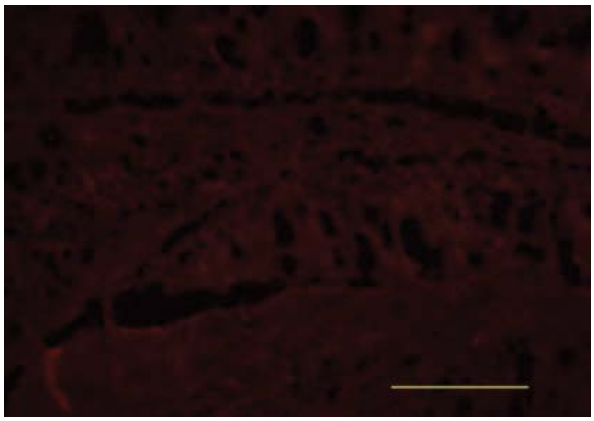

Figure 27: Aricept group IDE immunofluorescence.

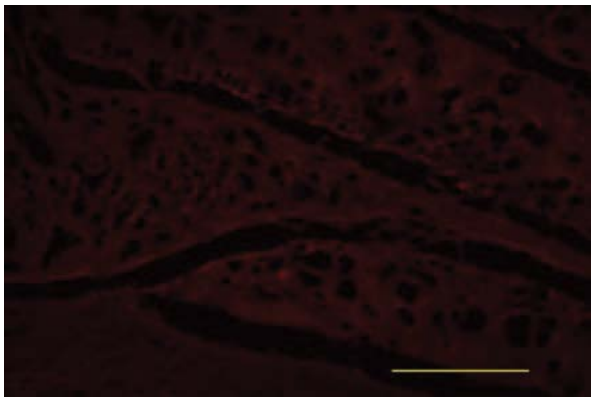

Figure 28: Xixin decoction group IDE immunofluorescence.

of AD and is sheared from β-amyloid precursor protein through the sequential actions of β and γ secretases [7]. Resulting Aβ fragments gather and form the final soluble oligomer, which has demonstrable neurotoxicity [8]. The oligomer mixture that is composed of Aβ42 can form a diffusible portion (ADDLS), which is its most toxic form. This neurovirulent substance is soluble and contains no fiber. Only a small amount of this substance can lead to damage of the mature neuron. Synaptic dysfunction and the oxidative stress response can produce various toxic effects for many types of neurons, including cholinergic ones as well as those located in the hippocampus. Moreover, both can also affect synaptic plasticity [9]. Past work has shown that Aβ oligomers can affect the postsynaptic density as well as the dendritic spine [10]. Moreover, *in vivo* work has shown that Aβ oligomers can immediately disrupt the formation of LTP, leading to problems with memory formation [11].

$BACE_1$ is β secretase [12], which is a primary, limiting enzyme that promotes the Aβ formation and causes age

pigment. Much research has shown that $BACE_1$ expression and enhancement of enzymatic activity are important molecular pathological characteristics for early phase AD. In current AD therapeutic research, the regulation of $BACE_1$ expression has been regarded as a major therapeutic target that could lead to efficient treatment effects [13,14].

IDE is a downstream, of metalloprotease insulin receptor that is expressed in all cells of the body. It is primarily localized in the cytoplasm, peroxisome and endosome and is predominantly expressed in the liver, muscles, and brain tissues. IDE typically functions as an extracellular receptor in the form of homocystein of thiolactone and as a dimer or trimer. In particular, the dimer form has high biological activities and can eliminate various peptide materials, including Aβ and insulin [15]. Furthermore, IDE can degrade Aβ under neutral conditions and prevent the formation of age pigment as well as eliminate Aβ neurotoxicity [16]. $Aβ_{42}$-the major ingredient of age pigment-is a substrate that is known to be degraded by IDE. Given this, IDE can play an important role in the formation of AD by adjusting the levels of Aβ degradation.

Our experiment found that when compared with the Model group, mice treated with Xixin had significantly shorter escape latencies in a Morris water maze test ($p < 0.05$). Moreover, they also had a significant increase in the frequency of platform crossings ($p < 0.05$). When compared with the Model and Aricept groups, Xixin treated mice had marked decreases in hippocampal neuronal degeneration. When compared with the Model groups, Xixin treatment resulted in reduction of Aβ42 expression in specific brain areas ($p < 0.05$). Xixin treatment also resulted in a significant decrease to BACE expression ($p < 0.05$) with a significant increase in IDE expression ($p < 0.05$).

Collectively, these result showed that Xixin treatment resulted in improvements to learning and memory in APP double transgenic mice. Moreover, it also had a protective effect on hippocampal neurons as well as their synaptic construction and function. Xixin treatment also reduced Aβ42 content in brain tissue of APP double transgenic mice and restrained IDE overexpression. Given these, we speculate that the mechanism of Xixin in improving AD learning and memory capabilities and preventing AD pathological process are through inhibition of BACE. This inhibition leads to a reduction in Aβ generation and promotion of brain IDE expression. Ultimately, this leads to acceleration in the degradation and elimination of Aβ42, reaching a relative balance between the generation and elimination of Aβ in the brain. However, the mechanism behind the actions of Xixin in reliving AD pathological progress will need to be researched further.

Author Contributions

Diwu Yong-chang was the project leader and was responsible for the project design, experimental scheme, and instruction during the experimental process. Cui Na performed statistical data analysis along with revisions and editing for the final manuscript. Gu Jie was responsible for molecular-biological indicator tests and image analysis. Gu Zan, Yang Ke, Zeng Jian, Li Xiang, Gao Yan-bin, Tang Xue-cheng, and Zhai Jia-ming were university postgraduates who were responsible for molecular biological detection.

Conflicts of Interest

The authors state that they have no conflicts of interest.

Funding

This study is funded by the National Natural Science Foundation of China (No.81373703; NO.81674042).

References

1. Holtzman DM, Morris JC, Goate AM (2011) Alzheimer's Disease: The Challenge of the Second Century. Sci Transl Med 3: 77.
2. Sang-Sun Yoon, Sangmee Ahn Jo (2012) Mechanisms of Amyloid-β Peptide Clearance: Potential Therapeutic Targets for Alzheimer's Disease. Biomol Ther (Seoul) 20: 245-255.
3. Hardy J, Selkoe DJ (2002) The amyloid hypothesis of Alzheimer's disease: progress and problems on the road to therapeuties. Science 297: 353-356.
4. Hook G, Yu J, Toneff T, et al. (2014) Brain Pyroglutamate Amyloid-Beta is Produced by Cathepsin B and is Reduced by the Cysteine Protease Inhibitor E64d, Representing a Potential Alzheimer's Disease Therapeutic. J Alzheimers Dis 41: 129-149.
5. Kazumi Motoki, Hideaki Kume, Akiko Oda, et al. (2012) Neuronal β-amyloid generation is independent of lipid raft association of β-secretase BACE1: analysis with a palmitoylation-deficient mutant. Brain Behav 2: 270-282.
6. Gong Y, Chang L, Viola KL, et al. (2003) Alzheimer's disease-affected brain: presence of oligomeric A beta ligands (ADDLs) suggests a molecular basis for reversible memory loss. Proc Natl Acad Sci U S A 100: 10417-10422.
7. Kang J, Lemaire HG, Unterbeck A, et al. (1987) The precursor ofAlzheimer's disease amyloid A4 protein resembles a cell-surface receptor. Nature 325: 733-736.
8. Sajadi A, Provost C, Pham B, et al. (2016) Neurodegeneration in an Animal Model of Chronic Amyloid-beta Oligomer Infusion Is Counteracted by Antibody Treatment Infused with Osmotic Pumps. J Vis Exp.
9. Guo Q, Wang Z, Li H, et al. (2012) APP physiological and pathophysiological functions: insights from animal models. Cell Res 22: 78-89.

10. Price KA, Varghese M, Sowa A, et al. (2014) Altered synaptic structure in the hippocampus in a mouse model of Alzheimer's disease with soluble amyloid-βoligomers and no plaque pathology. Mol Neurodegener 9: 41.

11. de la Monte SM, Wands JR (2008) Alzheimer's disease is type 3 diabetes:evidence reviwed. J Diabetes SCI Techol 2: 1101-1113.

12. Vassar R, Bennett BD, Babu-Khan S, et al. (1999) Beta-secretase cleavage of Alzheimer's amyloid precursor protein by the transmembraneaspartic protease BACE. Science 286: 735-741.

13. Russo C, Schettini G, Saido TC, et al. (2000) Neurobiology: Presenilin-1 mutations in Alzheimer's disease. Nature 405: 531-532.

14. Li Y, Zhou W, Tong Y, et al. (2006) Control of APP processing and Abeta generation level by BACE1 enzymatic activity and transcription. FASEB J 20: 285-292.

15. Hubin E, Cioffi F, Rozenski J, et al. (2016) Characterization of insulin-degrading enzyme-mediated cleavage of Aβin distinct aggregation states. Biochim Biophys Acta 1860: 1281-1290.

16. Zhao Z, Xiang Z, Haroutunian V, et al. (2007) Insulindegrading enzyme activity selectively decreases in the hippocampal formation ofcases at high risk to develop Alzheimer's disease. Neurobiol Aging 28: 824-830.

DOI: 10.36959/524/327 | Volume 1 | Issue 1